WooDowel: Enhancing Triboelectric Plywood Sensors with Electromagnetic Shielding

Yonghao Shi
Simon Fraser University
Burnaby, BC, Canada
yonghao_shi@sfu.ca

Chenzheng Li
Simon Fraser University
Burnaby, BC, Canada
cla429@sfu.ca

Yuning Su
Simon Fraser University
Burnaby, BC, Canada
yuning_su@sfu.ca

Xing-Dong Yang
Simon Fraser University
Burnaby, BC, Canada
xingdong_yang@sfu.ca

Te-Yen Wu
Florida State University
Florida, FL, USA
tw23l@fsu.edu

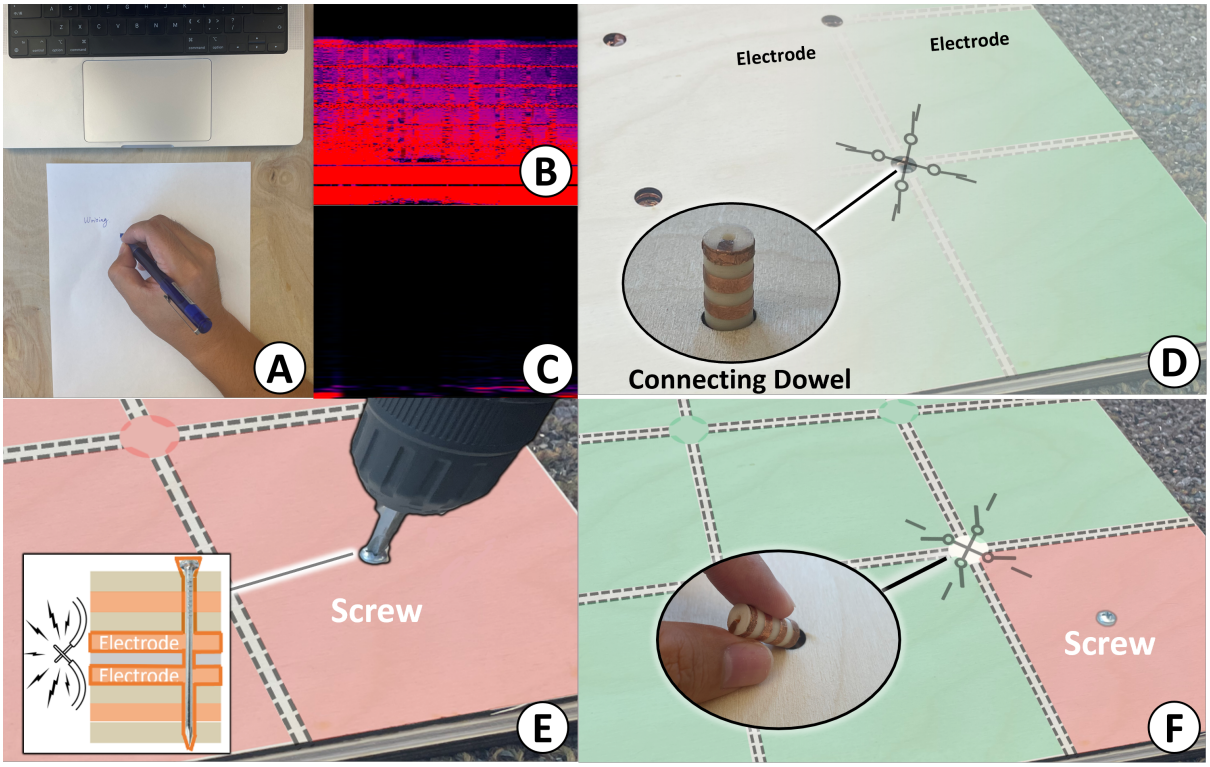

Figure 1: The illustration shows the impact of EM interference on the current design of the plywood vibration sensor, which operates based on the triboelectric effect. (A) A user is writing on the plywood sensor while a laptop emitting EM noises is placed on top of the sensor; (B) The signal from the sensor without any EM shielding, showing the interference caused by the nearby laptop; (C) The signal from the sensor with EM shielding, indicating that the interference has been reduced. Our design, called WooDowel, allows a user to manually 'turn off' a short-circuited electrode caused by the presence of a screw. (D) The electrodes of WooDowel are connected by specially designed dowels; (E) The entire sensor is short-circuited because a screw electronically connects the electrode layers; (F) The affected electrode can be manually disconnected from the rest of the sensor by removing the connecting dowel, allowing the sensor to remain functional.

ABSTRACT

We present a new approach to address the challenges associated with maintaining the functionality of triboelectric vibration sensors in smart plywood during woodworking operations involving nails and screws. The current state-of-the-art sensor design employs non-overlapping electrodes, which unfortunately leads to significant compromises in terms of signal strength and clarity, particularly in real-world scenarios that involve electromagnetic (EM) interference. To overcome these limitations, we propose a method that enables the woodworker to manually isolate short-circuited electrodes. This method facilitates the creation of sensors using overlapping electrodes, while also incorporating EM shielding, thereby resulting in a substantial improvement in the sensor's robustness when detecting user activities. To validate the effectiveness of our proposed approach, we conducted a series of experiments, which not only shed light on the drawbacks of non-overlapping electrode designs but also demonstrated the significant improvements achieved through our method.

CCS CONCEPTS

• **Human-centered computing → Interaction devices**.

KEYWORDS

Smart Environment, computational material, TENG

ACM Reference Format:

Yonghao Shi, Chenzheng Li, Yuning Su, Xing-Dong Yang, and Te-Yen Wu. 2024. WooDowel: Enhancing Triboelectric Plywood Sensors with Electromagnetic Shielding. In *Proceedings of the CHI Conference on Human Factors in Computing Systems (CHI '24), May 11–16, 2024, Honolulu, HI, USA.* ACM, New York, NY, USA, 17 pages. https://doi.org/10.1145/3613904.3642304

1 INTRODUCTION

Triboelectric vibration sensors use a structure comprising a triboelectric material layer sandwiched between two electrode layers to convert mechanical vibrations into electrical signals [28]. This simplistic structure allows for easy integration of these sensors into everyday materials such as paper [3] and plywood [30], thereby enabling the creation of objects with inherent vibration-sensing or power-harvesting capabilities [28]. While the integration process is straightforward, a significant challenge arises when designing these sensors for smart materials: ensuring their functionality even if a part of the sensor is damaged during the fabrication process. For instance, plywood vibration sensors must be able to withstand woodworking operations like sawing, nailing, or screwing, which are necessary for the assembly of household items. However, the traditional design of triboelectric vibration sensors makes them susceptible to malfunction when metallic elements such as screws and nails penetrate them, leading to short circuits between the two electrode layers (Fig. 2A).

To address this issue, one potential approach is to design the electrode layers in a way that avoids overlap with each other [30] (Fig. 2B). However, the non-overlapping design of the electrodes can significantly compromise the sensing capability of the triboelectric vibration sensors. In real-world scenarios, the sensor may be exposed to EM interference caused by electronic devices that are in direct contact with the sensor, such as a laptop placed on a smart desk, or even devices that are in proximity (Fig. 1A). This EM interference can have a significant impact on the sensitivity of the sensor. As shown in the result of our experiment, the average signal-to-noise ratio (SNR) of the sensor drops from 4.15dB to -1.16dB when the EM shielding is disabled. This significant reduction in SNR greatly affects the accuracy of the sensor in accurately recognizing user activities. Furthermore, the issue of picking up EM signals from nearby electronic devices poses an additional challenge, as it becomes difficult to accurately filter out the interactions occurring in the surrounding space. For instance, distinguishing whether the user is operating a jigsaw on the desk constructed using the plywood sensor or in a nearby space solely based on the sensor readings becomes challenging. To mitigate EM interference, a common solution is to sandwich the sensor between two insulation layers of conductive materials. This shielding mechanism can help minimize the impact of EM interference but it conflicts with the initial solution of avoiding electrode overlap (Fig. 2C).

In this paper, we propose an alternative method to address the challenges posed by the presence of nails and screws in triboelectric vibration sensors. Our approach involves manually isolating short-circuited electrodes from the rest of the sensor, accomplished by a woodworker 'turning off' up to three specially designed 'dowels'. By carefully separating the affected electrodes from the main body of the sensor, the functionality of the sensor can be preserved. While our method requires manual effort and results in a reduced sensing area, it offers two unique benefits over the existing solution. Firstly, it allows for the creation of triboelectric vibration sensors with overlapping electrodes. This feature ensures that the signal strength of the original sensor design remains intact, thereby maintaining sensitivity to a wide variety of user activities. Additionally, our method supports the incorporation of electromagnetic shielding into the sensor design. This shielding substantially improves the signal-to-noise ratio, leading to more robust recognition of user activities. By minimizing unwanted interference, the sensor can accurately detect the activities carried out in direct contact with it.

To validate the proposed approach, we developed a prototype (called WooDowel) with an array of square electrodes overlapping with each other. The electrical connections between the electrodes are established through the corners of the square using carefully designed connecting dowels. In cases where a connection needs to be disrupted to avoid short-circuiting, a regular wooden dowel can replace the connector. By replacing all the dowels in the neighbors, a compromised electrode could be isolated from the rest of the sensor. To ensure that woodworkers can easily incorporate this additional step into their established work routine, we also implemented a short-circuit detector. This detector can be connected to the sensor using another new type of dowel, which features a power jack interface specifically designed to facilitate wiring. When a nail

CHI '24, May 11–16, 2024, Honolulu, HI, USA

ACM ISBN 979-8-4007-0330-0/24/05…$15.00
https://doi.org/10.1145/3613904.3642304

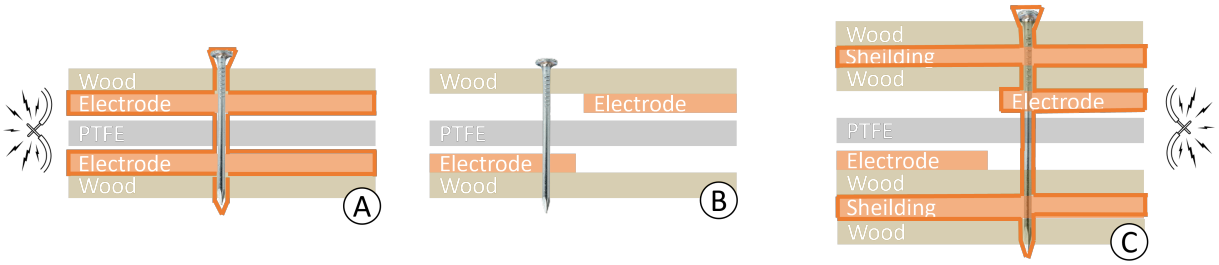

Figure 2: The existing triboelectric-based plywood vibration sensor faces issues when handling the presence of screws or nails. (A) In the case of an overlapping electrode design, a nail can create a short circuit by connecting the electrode layers. (B) To address this issue, a non-overlapping electrode design is employed in the state-of-the-art design, allowing the sensor to remain functional even when nails or screws are present. (C) However, if the non-overlapping electrode design is augmented with EM shielding, it becomes impossible to avoid the short circuit.

is inserted into the plywood sensor and a short circuit occurs, the detector promptly alerts the worker by activating a buzzer. Furthermore, to better inform the implementation of our prototype, we conducted studies to investigate the impact of plywood materials and their thickness on sensor signals. In a controlled experiment, we measured the sensing performance of a smart table made with our prototype by an experienced woodworker with 20 common work and kitchen activities (e.g., writing on a table). Our results indicated that the smart table achieved a recognition accuracy of over 90%.

The primary contributions of this research include: (1) study results that highlight the negative effects of a non-overlapping electrode design on the signal strength and clarity of triboelectric vibration sensors when used in a practical environment with EM interference; (2) a novel alternative approach that uses specially-designed dowels to maintain the functionality of triboelectric vibration sensors during woodworking operations, without compromising their signal strength and quality; and (3) the result of a study that assesses the recognition accuracy of our proposed approach in recognizing 20 common daily activities within an environment affected by EM noise.

2 BACKGROUND AND RELATED WORK

In this section, we will review previous research conducted in the areas of interactive wooden artifacts, sensors designed to withstand physical damage, and vibration sensing based on the triboelectric effect.

2.1 Vibration Sensing based on the Triboelectric Effect

Triboelectric vibration sensors operate on the principles of triboelectrification, the foundation of triboelectric nanogenerators (TENGs). TENGs are devices that can convert mechanical energy into an accompanying electrical response. This technology has gained significant attention in the field of energy harvesting due to its simple structure and remarkable efficiency in transferring energy at low frequencies [28]. The concept of triboelectrification involves generating electric charges through the contact and separation of two different materials. When these materials come into contact, electrons can transfer from one material to another, creating an imbalance in charge distribution. This generated charge difference can then be harnessed and utilized to produce electrical energy.

Typically, Triboelectric Nanogenerators (TENGs) are constructed using two layers of triboelectric materials, one positive and one negative, each connected to an electrode layer. This configuration allows for triboelectrification to occur, and the electrodes are responsible for harvesting the resulting energy. In an attempt to simplify the design, an alternative approach has been proposed. In this alternative design, only one electrode is attached to either the positive or negative triboelectric material. However, this modified design has been found to result in reduced power output from TENGs [19] and requires specific enhancements, such as integrating a spacer or undergoing chemical treatment, in order to improve energy harvesting [12].

In the research community, TENGs have shown great potential in converting low-frequency vibrations, commonly found in machinery, home appliances, and human movements, into electrical energy. One notable example is the wood-based TENG (W-TENG) proposed by Hao et al. [6], which effectively produces electric output for powering microelectronic devices. Building upon this concept, subsequent works by Kuntharin et al. [13] have further enhanced the energy harvesting capabilities of W-TENGs by chemically functionalizing wood materials as strong triboelectric materials. TENGs have also expanded their applications to various sensing domains, including pressure detection [10][16], vibration sensing [32][7], activity recognition [13], wind speed measurement[27] , disk rotation [15], and acceleration detection [35]. By integrating energy harvesting and sensing capabilities, TENGs can function as self-powered sensors, generating their own electricity to operate autonomously[28]. This unique feature sets them apart from other vibration sensors, such as piezoelectric ceramics or PVDF poled piezoelectric films, as triboelectrification-based methods are more affordable and simpler to produce [33], making them highly suitable for large-scale manufacturing and widespread applications.

2.2 Interactive Household Items Made of Wood

Wood is a preferred choice for furniture, utensils, and decorative items. However, with the advancement of technology, wood has also found its way into the realm of interactive objects and household items, which incorporate sensors and/or computational elements. Existing research in this field has predominantly focused on attaching sensing devices to pre-existing wooden furniture or artifacts [6][13][14][34][11][5][22]. For example, studies have explored the use of embedded vibration sensors in tables, walls, and floors to detect touch or gesture events [8][21][31][30] , as well as activities such as cutting, typing, and walking[25]. Other research has aimed at detecting the presence of daily items on a table or even individuals falling on the floor[23] . While these approaches effectively introduce interactivity to the environment, they often require customization, such as sensor placement optimization, for new objects, limiting their practicality. In contrast to these conventional approaches, iWood [30] and Woodowel has emerged as an interactive material based on the triboelectric effect. Their sensing capabilities are more consistently distributed across the entire material. They can be directly inherited by any object made from interactive materials, regardless of the specific processing methods employed during its fabrication. By leveraging this inherent property, interactive materials offers a more holistic and consistent solution for integrating interactivity into wooden objects.

2.3 Sensors Designed to Withstand Physical Damage

Traditional sensor research had a limited emphasis on designing sensors that could maintain functionality even when physically damaged. However, with the growing demand for supporting rapid prototyping hardware devices, researchers have begun exploring alternative sensor designs for interactive systems. One notable advancement in this area is the development of cuttable sensors, exemplified by the touch sensing strip created by Wimmer et al.[29] and Holman et al. [9]. This strip can be cut into various lengths to meet different application requirements. Additionally, Dementyev et al. [2] designed a sensor tape that can be cut into different lengths to detect sensor deformation and measure proximity to nearby objects. Expanding beyond one-dimensional cutting, Olberding et al. [20] introduced a multi-touch sensor sheet that can be cut into various 2D shapes. To ensure the sensor's durability against damage caused by cutting, the authors devised a novel electrode layout based on insights from physical routing topologies. A study involving six cutout shapes showed that the new electrode design allowed 80% of the electrodes to remain functional after cutting. Building upon this research, Takahashi et al. [26] developed a cuttable coil grid using an H-tree-based method. Their work showcases the potential for extending the concept of cuttable sensors beyond traditional sensor applications into areas such as wireless power transmission.

In contrast to the focus on cutting in the aforementioned research, Wu and Yang redesigned the triboelectric vibration sensor to address the malfunction caused by short circuits resulting from metallic screws and nails penetrating the electrode layers embedded in a plywood panel [30]. Building upon their work, our research aims to address one of the most significant challenges affecting the practical utility of their sensor redesign. Specifically, we demonstrate the reduction in signal and power generated by their sensor designs and the substantial impact on sensing performance due to the presence of EM noise. Additionally, we propose a novel approach to tackle the problem introduced by the presence of nails and screws, while concurrently preserving the sensor's ability to shield against EM interference.

3 EXPERIMENTS: UNDERSTANDING THE EFFECTIVENESS OF THE EXISTING DESIGNS

We conducted a series of experiments to evaluate the effectiveness of the existing designs of triboelectric vibration sensors for interactive plywood. Specifically, we focused on quantifying three key aspects: (1) the impact of non-overlapping electrode design on signal strength, (2) the impact of EM noise on sensor signals, and (3) the vulnerability of the sensor, in the absence of EM shielding, to nearby electronic devices.

3.1 Experiment 1: The Impact of Non-Overlapping Electrode Design

The goal of this experiment was to assess the impact of the current design of the non-overlapping electrodes on the strength of the signals. Specifically, the study aimed to examine the tradeoff resulting from modifications made to the original electrode design in order to improve the sensor's ability to withstand woodworking operations.

3.1.1 Apparatus. We replicated the design of iWood on a small piece of plywood, following the implementation details described by Wu and Yang [30]. The prototype consisted of a 0.2mm thin polytetrafluoroethylene (PTFE) film, sandwiched between two layers of 0.1mm in thin copper film, which were then bonded to a substrate of plywood board ($100mm \times 100mm \times 12.7mm$) on each side. Each electrode measured $50mm \times 50mm$ wide, covering half of the PTFE film on each side. To provide a basis for comparison, we also implemented a second prototype with overlapped electrodes. In this configuration, both electrodes covered the entire sensing area. The sensor data was measured using a digital oscilloscope from Keysight (model DSOX2004A) with a sampling rate of 10 kHz.

3.1.2 Data Collection. We performed a weight-dropping task to measure the sensor signals of the two prototypes. This task aimed to induce consistent mechanical vibrations on the sensor's surface. Each trial involved dropping a weight of 50 g from a height of 5 cm, and this process was repeated 28 times. We measured the peak-to-peak value as the sensor's signal strength for each trial. To ensure accuracy and consistency in the free-fall of the weight for each trial, we employed a fixed pulley system. This system allowed us to lift the weights to the desired height, ensuring a uniform and controlled drop every time.

3.1.3 Result. Our result shows that the use of non-overlapping electrodes resulted in a notable reduction in signal strength, with an average value of 0.7V (std: 0.45). In comparison, the prototype featuring overlapping electrodes yielded a substantially higher average signal strength of 1.25V (std: 0.74). The signal strength of the TENG sensor is a critical factor in assessing its susceptibility to

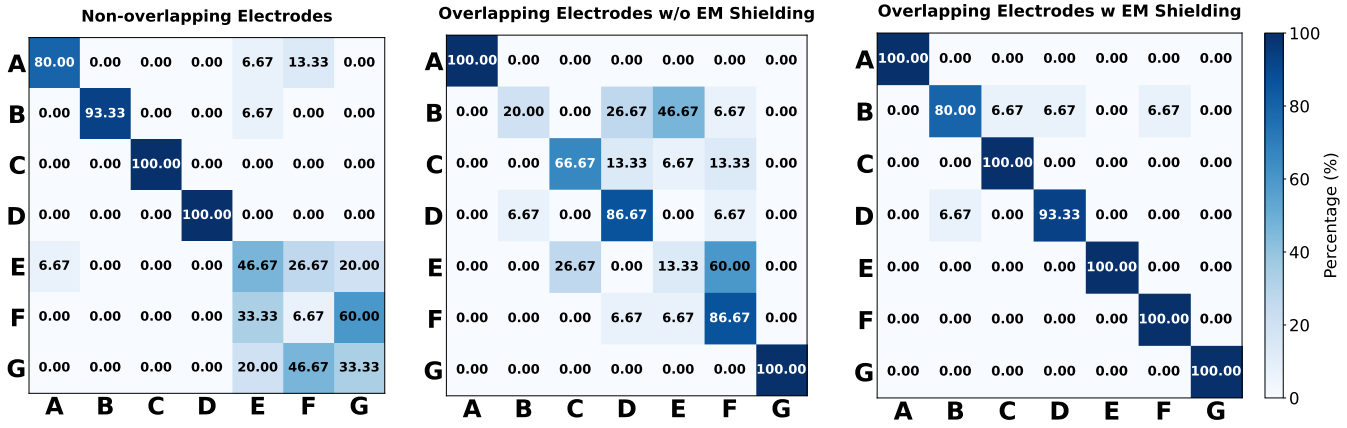

Figure 3: The confusion matrix showing the results of our study in three conditions. Left: non-overlapping electrodes; Middle: overlapping electrodes without EM shielding; Right: overlapping electrodes with EM shielding. (A) Vacuum, (B) Drill, (C) Sander, (D) Jigsaw, (E) Kettle, (F) Speaker, (G) Background

EM interferences emanating from nearby electronic devices. The weakened signal in the non-overlapping electrode design introduces potential issues, specifically a decreased signal-to-noise ratio (SNR). This compromised SNR leaves the system more vulnerable to disruptions due to EM interference, thus compromising the sensor's effectiveness in accurately sensing various user activities. To further investigate this, we conducted the next study.

3.2 Experiment 2: The Impact of EM Noise

This experiment aimed to evaluate the impact of EM noise on SNR and, consequently, the recognition performance of the vibration sensor. Our findings from Experiment 1 have suggested that the non-overlapping design of the sensor electrodes resulted in a significant decrease in signal strength. However, the impact of this decrease on the accuracy of activity recognition remains unclear. Therefore, to investigate the effect of EM noise, we opted to incorporate both overlapping and non-overlapping electrode (iWood) designs into our study.

3.2.1 Apparatus. Our prototypes in this study were similar to those used in Experiment 1. However, in order to accommodate the activities conducted during the study, we created a larger version that measured 600 mm in length and 300 mm in width. This ensured an adequate sensing space for the various tasks involved in the research. Furthermore, we developed another prototype that incorporated the overlapping design of the electrodes but with the inclusion of EM shielding. To implement the EM shielding, we positioned the vibration sensor between two grounded copper layers. An extra plywood layer was also introduced to serve as a separator between the shielding layer and the sensor electrodes. To maintain a consistent thickness between the three prototypes (25.4 mm), all four plywood layers used in this prototype were uniformly 6.35 mm thick. We used a laptop (Alienware M18 R1) as the source to introduce EM interference into the experimental setup, placing it on top of the sensor.

3.2.2 Activities and Data collection. We measured the performance of the sensors using the vibrations produced by six different types of electronic devices. These devices included a handheld vacuum cleaner, electronic sander, electronic drill, jig saw, electric kettle, and speaker (playing drum music). Note that electronic devices emit EM signals as a byproduct of their operation. Our tests revealed a significant correlation between these EM signals and the vibration signals emitted by the devices. When these two signals are superimposed, the captured signals from electronic devices become more pronounced. With the inclusion of electronic devices in our study, we created a scenario that slightly favored the non-overlapping design. This allows our study results to be considered as the upper boundary of performance for the non-overlapping design. To simulate real-world usage scenarios, we operated the sander, drill, and saw on a piece of wood that was placed on top of the sensor. However, for all other devices, we directly operated them on top of the sensor. Each activity was repeated 15 times, with the order of activities and the repetitions randomized. The laptop was placed on one of the corners of the sensor. To account for variations in location, the tested devices were randomly positioned within the free space of the sensor during the data collection process. In addition to the six devices, we also included an empty class consisting solely of background noise in our classifier. The signal processing, featurization, and machine learning procedures were consistent with those described in the iWood study [30].

3.2.3 Result. The results of our study indicate that the implementation of EM shielding greatly enhances the performance of the plywood vibration sensor. Specifically, when equipped with EM shielding, the average SNR of the sensor with overlapping electrodes was found to be 4.15 dB. In contrast, the same type of sensor without EM shielding exhibited a much lower average SNR of -0.43 dB. The sensor with non-overlapping electrodes and without EM shielding (iWood) had the lowest SNR value of -1.16 dB. Furthermore, in terms of activity recognition, the system achieved an accuracy rate of 96.1% (std: 7.55) when using the sensor with overlapping electrodes and EM shielding. On the other hand, the same type of sensor without EM shielding yielded a significantly lower overall accuracy rate of 67.62% (std: 19.37). The sensor with non-overlapping electrodes and without EM shielding had the lowest

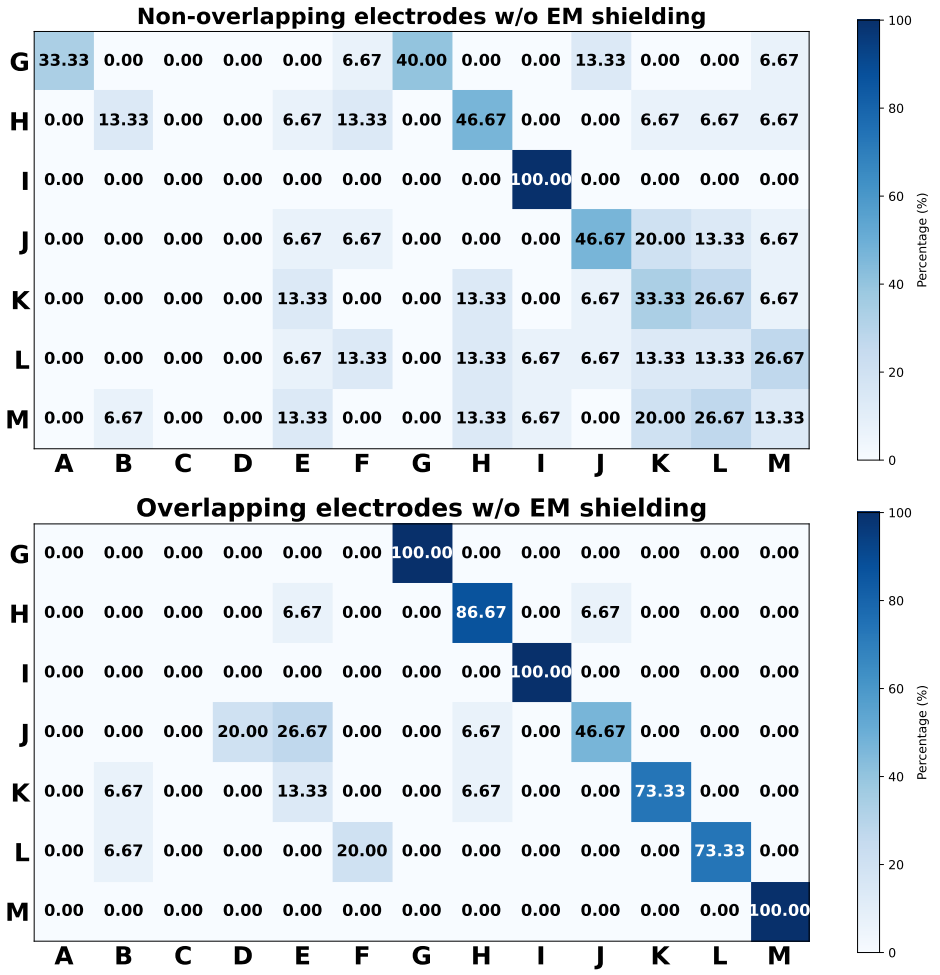

Figure 4: The confusion matrix showing the results of our study with non-contact (NC) and contact-based events in the two conditions without EM shielding. Top: non-overlapping electrodes. Mid: overlapping electrodes. No false positive was observed in the condition with EM shielding. (A) Vacuum, (B) Drill, (C) Sander, (D) Jigsaw, (E) Kettle, (F) Speaker, (G) Vacuum(NC), (H) Drill(NC), (I) Sander(NC), (J) Jigsaw(NC), (K) Kettle(NC), (L) Speaker(NC), (M) Background

accuracy rate of 63% (std: 37). The confusion matrix of the results can be seen in Fig. 3. These findings highlight the substantial benefits of incorporating EM shielding into the triboelectric vibration sensor. Not only does it improve the SNR, but it also significantly enhances the accuracy of activity recognition. This indicates that the addition of EM shielding is a crucial factor in optimizing the performance of the sensor. Additionally, these findings provide further evidence of the significant trade-off in sensing capability made by the non-overlapping design of the electrodes.

3.3 Experiment 3: The Impact of Nearby Electronic Devices

The goal of this experiment was to evaluate the vulnerability of the sensor to nearby electronic devices. It is important to note that an operating electronic device near the sensor emits EM signals that may mistakenly be detected by the sensor. This can result in the sensor falsely indicating activity in contact with it. For example, if a user is using a jigsaw to cut a piece of wood on the floor near a smart table, the EM signals produced by the jigsaw may be mistakenly identified as the jigsaw operating on the smart table. Such false positives can significantly impact user experience, as the sensor is unable to correctly interpret user interactions. Therefore, the main focus of this study was to measure the effectiveness of EM shielding in effectively filtering out the interference caused by electronic devices that are not in direct contact with the sensor.

3.3.1 Apparatus. The experimental setup used in this study was the same as the apparatus employed in Experiment 2.

3.3.2 Activities and Data collection. In this study, we used the same set of electronic devices as those used in Experiment 2. However, instead of directly placing the devices directly on top of the sensor, we operated them near the sensor without any physical contact. Specifically, the kettle and speaker were positioned on a separate

desk near the sensor, while all the other devices were manually held above the sensor. To minimize potential confounding effects, EM interference was excluded from this experiment (i.e., the laptop used in Section 3.2). Similar to Experiment 2, each activity was repeated a total of 15 times, with both the sequence of activities and the repetitions randomized. To assess the extent to which non-contact activities are incorrectly identified by the system as contact-based actions, we incorporated the data obtained from Experiment 2. As a result, our classifier had a total of 13 classes. To evaluate the performance of the various sensor designs, we employed the same signal processing and machine learning techniques as in previous experiments.

3.3.3 Result. The study's findings reveal that the sensor without EM shielding, but with non-overlapping electrodes (iWood), exhibited an average false positive rate of 20%. On the other hand, the sensor with overlapping electrodes, but without EM shielding, demonstrated a slightly lower false positive rate of 14.3%. This suggests that many activities performed without direct contact with the sensor were mistakenly identified as actions occurring on top of the sensor (see Fig. 4). Importantly, this misidentification was not caused by the interference from the EM noise of the laptop. In the condition where EM shielding was used, no false positive was observed.

3.4 Discussion

The findings obtained from these experiments provide evidence of a significant compromise that arises from the existing designs in triboelectric vibration sensors. This compromise is necessary in order to ensure the sensor's durability during woodworking operations. However, it is important to note that the adoption of this non-overlapping design introduces more substantial concerns, specifically: (1) reduced signal strength; and (2) the inability to integrate EM shielding. As illustrated by the findings of Experiment 2 and Experiment 3, the absence of EM shielding can give rise to substantial issues in accurately identifying user activities and the failure to capture relevant contextual information in real-world usage scenarios where EM interference is prevalent. These findings shed light on the limitations of the current non-overlapping design of the electrodes. While effective in safeguarding the sensor against woodworking operations, it hampers the ability to incorporate EM shielding.

4 WOODOWEL

We propose an alternative approach to enable the plywood-based triboelectric vibration sensor to withstand the presence of screws and nails without compromising its original overlapping electrode design. Our primary objective is the preservation of the plywood sensor's ability as a material for creating diverse objects. This requires the sensor to be able to accommodate screws or nails within the sensing area without making assumptions about their location and characteristics, such as length or coating, which may vary across different projects. Thus, ad-hoc solutions such as electrode patterns specifically designed to avoid screws or nails at predetermined locations are unsuitable for our objective. In this section, we present the details of our proposed approach to resolve this issue.

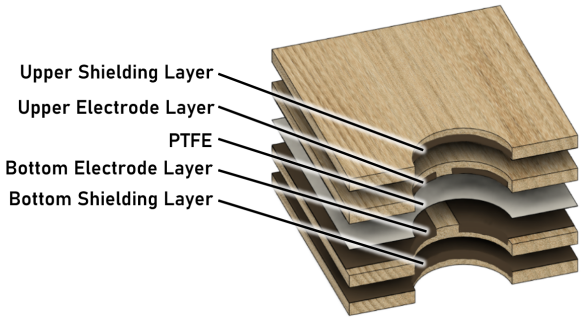

Figure 5: The structure of WooDowel.

The design of our plywood sensor closely resembles the prototype used in Experiment 3. It features overlapping electrodes that are enclosed within layers of EM insulation, which are then sandwiched between plywood substrates (Fig. 4). However, there is one notable difference in the design. Instead of utilizing a single continuous electrode, we have arranged the electrodes in a grid layout (see Fig. 6A). In this grid layout, each square electrode is interconnected to its neighboring electrodes through the corners. These connections on the corners can be selectively deactivated, allowing a short-circuited electrode to be isolated from the rest of the sensor. However, in the unlikely scenario of a nail or screw being inserted between two adjacent electrodes, it would still establish an electrical connection between the neighboring electrodes. To prevent such unintended electrical connections from occurring along the shared edges, the spacing between the electrodes has been set at a width of 4mm (Fig. 6A). This dimension has been carefully selected based on the largest wood screw diameter we found in the market.

Electrode isolation. To facilitate the disconnection of the electrodes, we implemented a simple switching mechanism using specially designed dowels, which are commonly used tools for joining wooden components. In our design, the connection between the electrodes is established by inserting a *Connecting Dowel* into a hole (Fig. 6C). This hole is on the path that connects the adjacent corners of the electrodes (Fig. 6B). The connecting dowel is specifically designed to connect all the neighboring electrode layers. As a part of the plywood sensor, the connecting dowels come pre-inserted. This means that when the sensor is assembled, the connection between the electrodes is already established. However, if there is a need to disable a connection, a connecting dowel can be easily removed by pushing it out using a screwdriver and replaced with a regular wooden dowel (Fig. 6E). If all connections to neighboring electrodes (up to a maximum of four connecting dowels) are disabled, the electrode can be completely isolated from the rest of the sensor. This provides the ability to individually disconnect specific electrodes as needed. Given the negligible impact of the size and shape of the sensing area on the sensing capability of the rigid triboelectric vibration sensor [18], the removal of short-circuited electrodes has minimal effects on the overall performance of the sensor beyond the reduced sensing area.

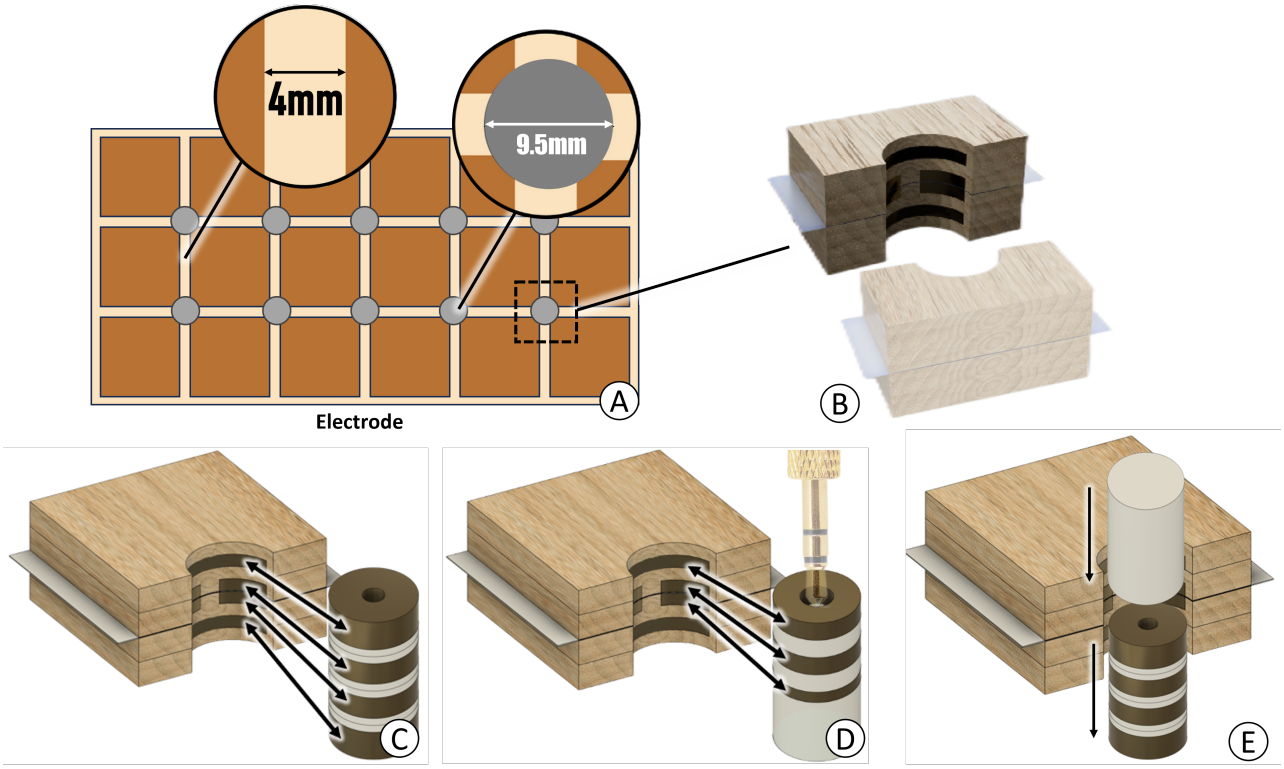

Figure 6: An illustration of our design of WooDowel and dowels. (A) The electrode layout of WooDowel; (B) The inside view of a hole that accommodates the connecting dowel, revealing the presence of dark stripes, which are made of conductive materials; (C) The connecting dowel and its connection inside the hole; (D) The power jack dowel and its connection inside the hole; (E) Replacing the connecting dowel with a wooden dowel results in the disconnection of the adjacent electrodes.

Grounding and wiring. To achieve effective EM shielding, it is crucial for the shielding layers to be properly grounded. This involves electronically connecting the two layers and wiring them to a ground source. However, the challenge arises when dealing with shielding layers embedded within plywood, as accessing these layers for wiring purposes becomes difficult. Furthermore, the sensor panel used to create furniture components is typically cut into smaller pieces during the woodworking process. This means that the grounding wiring can only be done after the panel has been cut into the desired shape. One possible approach is to wire through an open edge of the panel, but this solution is neither reliable nor practical in real-world scenarios. It requires woodworkers to possess additional knowledge and skills in electronics, which adds complexity and potential impracticality to the process.

To address this issue, we modified the design of Connecting Dowel to enable it to connect the two shielding layers. However, the current solution still lacks providing easy access to the layers from external computing devices for data processing. To overcome this limitation, we created a *Power Jack Dowel*, which offers convenient access to the connected shielding layer through a power jack (Fig. 6D). This allows for easy connection of the shielding layers to the ground through an audio jack. In addition to grounding, the Power Jack Dowel also provides convenient access to the electrode layers, enabling easy connection of the entire sensor to a microcontroller for data processing. The Power jack dowels can be pre-inserted into the plywood panel or inserted by a woodworker, replacing existing connecting dowels, once the desired panel shape has been cut. It is important to note that for each panel to function effectively, at least one Power Jack Dowel is required.

Notifying users a short circuit. We are aware that the manual disconnection of electrodes introduces an additional task into the established woodworking routines. Although it may not require significant physical effort, it can impose an additional cognitive burden on woodworkers, who must remember to disconnect the affected electrode after each insertion of a nail or screw. To address this issue, we developed a notification mechanism to alert users in the event of a short circuit. Specifically, we designed a compact device capable of detecting short circuits and emitting a buzzing sound upon detection (Fig. 8). To activate this device, users can simply connect it to the power jack dowel using a 3.5mm 3-pole audio jack.

4.1 Dowel Hole

Access to the conductive layers was made through the dowel holes. However, establishing a reliable electrical connection to the thin copper films has posed a significant challenge due to the limited

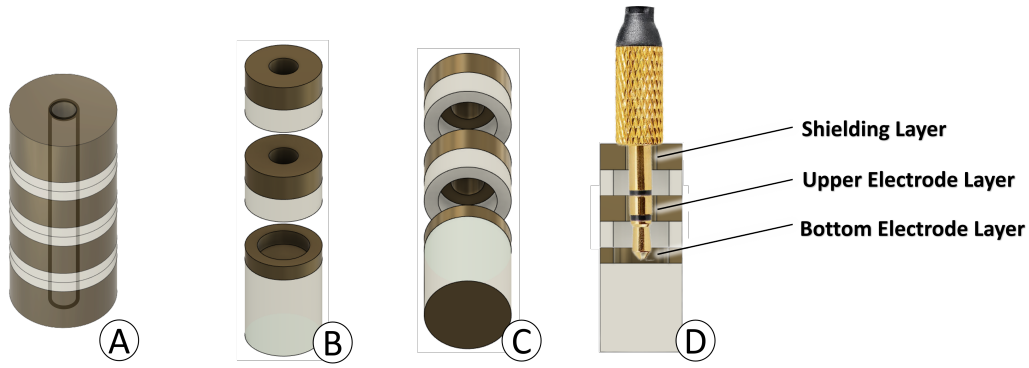

Figure 7: An illustration of the design of the connecting dowel and power jack dowel. (A) The 3D model of the connecting dowel, with a conductive path within the dowel that connects the two ends. (B) The breakdown of the 3D model of the power jack dowel from a 45-degree top-down viewing angle. (C) The 3D model of the power jack dowel from a 45-degree bottom-up viewing angle. (D) A diagram illustrating the connection of an audio jack to the power jack dowel.

contact area available across their cross-sections. To address this issue, we have enlarged the contact area by extending the copper films to the interior surface of the hole (Fig. 6B). Note that each dowel hole is strategically placed at the corner of four neighboring electrodes, ensuring access to both the shielding layers and electrode layers for all four electrodes. Therefore, on the inner surface of the dowel hole, the copper films for each individual electrode were separated to prevent any undesired connection between them (Fig. 6B).

4.2 Connecting Dowel

The Connecting Dowel serves the purpose of establishing a connection between the two shielding layers and the electrode layers of neighboring electrodes. It is created using a non-conductive material, with the exception of two conductive rings positioned near the middle of the dowel. These rings facilitate contact with the extended copper films of the top and bottom electrode layers (Fig. 6C). The top ring, with a width of 3.5 mm, is designed to connect the four adjacent electrodes situated above the PTFE film. Similarly, the bottom ring, also 3.5 mm wide, is responsible for connecting the four electrodes located below the PTFE film. These rings are spaced apart by a 1mm gap. It is important to note that the terms "top" and "bottom" are used solely for descriptive purposes in our design. Our implementation of the dowels, including the ones described below, does not have a specific direction or polarity.

To enable the connection between the two shielding layers, two additional conductive rings are incorporated at the ends of the connecting dowel. These rings, each with a width of 4.5 mm, at its two ends. These rings are designed to establish contact with the extended copper films of the top and bottom shielding layers. In order to effectively connect the two shielding layers, it is essential to establish an electrical connection between these rings. This is achieved by creating a conductive path within the dowel that connects the two ends (Fig. 7A). The rings and conductive path are connected through the tip of the dowel. The tip is covered with a non-conductive material to isolate the connections from the external environment.

4.3 Power Jack Dowel

The power jack dowel serves as an important component in facilitating access to each individual electrode layer and both shielding layers. Designed to be compatible with a 3.5mm 3-pole audio jack, the power jack dowel has three conductive rings on its exterior surface. These rings are positioned to establish contact with the top shielding layer, top electrode layer, and bottom electrode layer, respectively, from the top to bottom of the dowel (Fig. 7D). Internally, the power jack dowel has a 14 mm long hollow channel, designed for the insertion of an audio jack. Within this channel, there are two conductive rings, each connected to its corresponding outer ring on the top and middle sections of the dowel (Fig. 7B, C, D). These inner rings serve to establish connections with the corresponding poles of the audio jack. Furthermore, the bottom of the channel is connected to the bottom ring on the outside of the dowel. This connection facilitates the connection between the bottom electrode layer and the tip of the audio jack.

4.4 Short-Circuiting Detector

The short-circuit detector used in our system is a simple buzzer circuit consisting of a 3V buzzer and a protection resistor connected in series (Fig. 8). This circuit is powered by a button cell and can be activated or deactivated through a switch. The occurrence of a short circuit typically arises from the connection between the electrode and shielding layers or the connection between the two electrode layers caused by a nail or screw. In such instances, the buzzer circuit is close-looped, triggering the activation of the buzzer and generating an audible sound. To facilitate easy switching between the two states, a switch is used in the circuit. However, once the affected electrode is isolated from the rest of the sensor, the buzzer circuit is open, leading to the deactivation of the buzzer. Note that it is advisable to position the short-circuit detector away from areas where nails and screws are commonly used, such as the corners of tabletops where legs are connected, to avoid it being a part of the affected electrode.

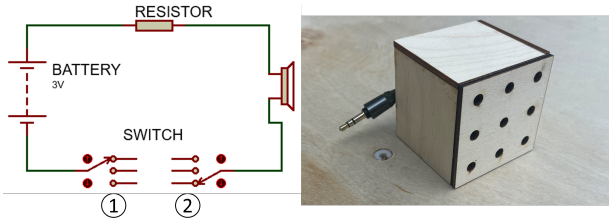

Figure 8: Left: The schematic diagram of the short circuit detector. Right: the implementation of the detector enclosed within a small 3cm cube box constructed out of plywood.

4.5 Electrode Size vs Sensing Area

The size of the electrode can have an impact on the sensing area of a sensor. Larger electrodes have a higher ratio between the electrode space and the gap space, which leads to more coverage. On the other hand, smaller electrodes are preferred because they result in less loss of sensing area in the event of short circuits. Ideally, an optimized electrode size would strike a balance between signal strength and sensor coverage when removing affected electrodes. However, the issue is that different item surfaces of varying sizes may require different optimization results. Additionally, the number of affected electrodes that need to be removed also affects the optimization outcome. In the case of a desktop surface of a given size, the optimal electrode size is determined by maximizing the ratio between the total area covered by the functional electrodes and the overall area covered by all electrodes, including both isolated and functional ones. Specifically, for a tabletop assembly with four legs, where a minimum of four electrodes on the tabletop will be damaged, the optimal electrode sizes for tabletops measuring $600mm \times 600mm$, $1000mm \times 1000mm$, and $1600mm \times 1600mm$ would be 85mm, 138mm, and 166mm, respectively. Therefore, it is clear that there is no universal optimal electrode size. According to this finding, the electrode size predetermined when creating the plywood sensor as a material is unlikely to be optimal to achieve the largest sensing area once the panel is cut into a smaller size based on the needs of a project. However, it is worth noting that the impact of using a non-optimized electrode size is relatively small, as suggested by our tests. For instance, for item surfaces ranging from 600mm to 1600mm wide, within a ±20mm range of the optimal sizes mentioned above, the change in the overall sensor coverage area is less than 5%. Therefore, for our implementation of the plywood panel, which is 1200mm wide, an electrode size falling within the range near the lower half of 138mm to 166mm could, in principle, lead to sensor coverage near its optimal value for desk surfaces ranging from 1000mm to 1600mm (by combining several pieces cut from the 1200mm panel). In our implementation, we selected an electrode size of 150 mm because it can be evenly divided by 1200mm.

5 UNDERSTANDING THE IMPACT OF PLYWOOD MATERIAL AND THICKNESS

When implementing our prototype, it is important to take into consideration various factors that can potentially impact signal strength. In particular, the material and thickness of the plywood substrate are significant factors to consider. However, the current body of literature lacks in-depth insights into the specific influence of these factors on signal strength. Therefore, we conducted two studies aimed at examining the effects of plywood material and thickness on signal strength.

5.1 How Plywood Material Impact Sensor Signals?

Intuitively, it is expected that plywood composed of materials with higher density would facilitate the transmission of vibration energy, while plywood made of lower density materials may potentially dampen the propagation of vibration energy. However, the precise impact of the various plywood materials available on sensor signals remain uncertain. In our study, we considered two common classifications of plywood provided by The Wood Database [17]: hardwood plywood and softwood plywood. Additionally, we included medium-density fiberboard (MDF) in our study, as it closely resembles plywood and is often used as a substitute for plywood.

5.1.1 Apparatus and Data Collection. We developed three plywood sensors using hardwood plywood, softwood plywood, and MDF. Each prototype had dimensions of $100mm \times 100mm \times 25.4mm$. Similar to Experiment 1, we conducted a weight-dropping task to record the sensor signals. In each trial, a weight of 50 g was dropped from a height of 5cm onto a randomly selected position within the sensor. We collected a total of 28 samples for each condition.

5.1.2 Results. The results of our study indicate that hardwood, MDF, and softwood plywood exhibit different average output signal strengths of 1.25 v, 1.15 v, and 0.77 v, respectively (Fig. 9). Our t-test showed a significantly higher signal strength observed from the hardwood compared to that of softwood ($p < 0.05$). This finding suggests that softwood plywood may have limitations in terms of its applications, although further investigation is necessary to confirm this finding. Furthermore, there was no significant difference between MDF and hardwood ($p = 0.59$), which can be attributed to their similar material density. These findings provide useful insights into the influence of three commonly used plywood materials on signal strength. Given that we do not have any specific material preference for this project, we have chosen to use hardwood for the remainder of our implementation in order to optimize signal strength.

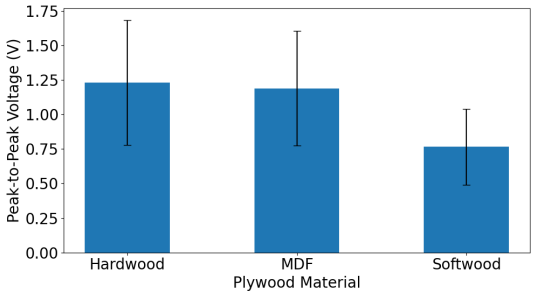

Figure 9: Peak-to-peak voltage shown by plywood material.

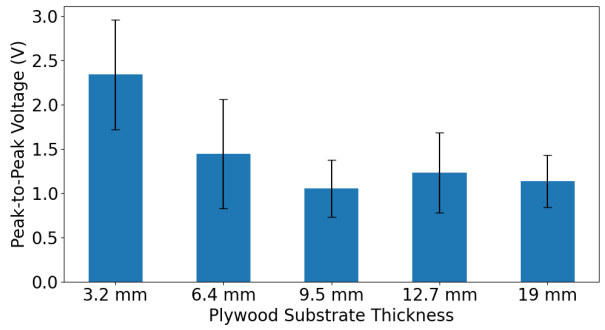

Figure 10: Peak to peak voltage shown by plywood substrate thickness.

5.2 How Substrate Thickness Impact Sensor Signals?

The goal of this study was to examine the impact of plywood substrate thickness on sensor signals. Prior to conducting the study, we conducted a market survey to gain a preliminary understanding of the thickness of common furniture, particularly tables, shelves, and floors, used in homes and workplaces. The data for this survey was collected from popular retailers such as Amazon and IKEA, focusing on best-selling plywood items. A total of 300 data points were collected for analysis. The findings of our survey revealed that the common thickness of household furniture made from plywood ranged from 12.7 mm to 38.1 mm. This corresponds to a substrate thickness of approximately 6.4 mm to 19 mm on each side of our sensor, respectively. This information guided our selection of thickness levels to be examined in the study. Specifically, we opted to investigate thickness levels of 6.4 mm, 9.5 mm, 12.7 mm, and 19 mm, covering the majority of wood panel models available in the market. In addition to this common thickness range, we were also interested in assessing signal strength on thinner substrates. Hence, we included an additional level of 3.2 mm.

5.2.1 Apparatus and Data Collection. We developed four plywood sensors, each incorporating a substrate of varying thickness as mentioned earlier. To enhance the signal strength, we opted for hardwood plywood as the substrate material. Note that the substrate on each side of the sensor consisted of two separate pieces that were attached to each other. This arrangement was necessary to incorporate EM shielding. The dimensions of the tested prototypes were kept consistent with those used in the material study. Similarly, to collect data for our study, we employed a weight-dropping test method.

5.2.2 Results. The findings of our study suggest that there is no linear correlation between the thickness of the substrate and the strength of the signal (Fig. 10). Although the thinnest condition of 3.2 mm yielded the highest output voltage, the signal strength obtained from the other tested thickness levels appeared to level off. This indicates that further decreasing the thickness beyond 3.2 mm does not result in a significant improvement in signal strength. Additionally, the observed differences in signal strengths between the substrates of 6.4 mm, 9.5 mm, 12.7 mm, and 19 mm thickness were relatively small. These findings imply that within the range of most tested thicknesses, the influence of substrate thickness on signal strength is minimal. Considering that our survey results indicate that over 70% of household furniture uses plywood panels of 25.4 mm or thicker, we opted for this dimension in our final implementation..

6 IMPLEMENTATION

In this section, we will present the implementation details of our approach, which is based on the designs of the plywood sensor discussed earlier.

Plywood sensor. Our interactive plywood material was constructed using four plywood substrates made of birch. Each substrate was measured to be 1200 mm by 1200 mm by 6.35 mm, resulting in a final sensor thickness of 25.4 mm (Fig. 11C). To create the electrodes, we used copper tape that was 150 mm wide. We also utilized copper tape for the shielding layers. In order to create dowel holes at the intersections of the electrodes, we used a drill with a diameter of 9.5 mm. To ensure precision and accuracy, a drill guide was used. This guide helped us maintain a vertical direction while drilling. To assemble all the different pieces together, we employed a bonding approach similar to the one described in iWood [30]. Once all the pieces were assembled, weights were placed on top of the structure and left undisturbed for a period of 24 hours. This allowed sufficient time for the glues to dry completely.

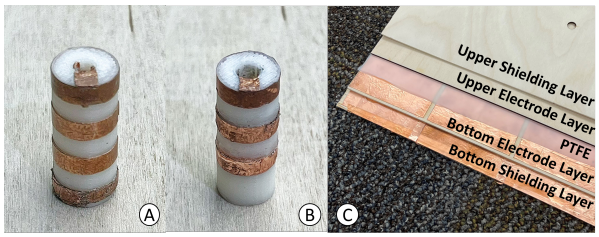

Figure 11: WooDowel prototype. (A) The connecting dowel; (B) The power jack dowel; (C) The breakdown of our plywood sensor prototype.

Dowels. All of the dowels mentioned above were fabricated using a 3D printer and PLA filament. Each dowel was printed with a height of 25.4 mm and a diameter of 9.4 mm. In the case of the connecting dowel, a conductive path was created through a tunnel with a dimension of 1 mm, which connects the two ends of the dowel (Fig. 11A). Additionally, all connecting dowels' holes could be concealed with a veneer to obscure the holes from external view. On the other hand, the power jack dowel consisted of three components stacked on top of each other (Fig. 11B). These components were responsible for establishing the connection between the pole of an audio jack and its corresponding copper layer within the sensor. To create the conductive rings and paths, copper tape was applied to the appropriate sections of the dowel. Our preliminary testing suggested that the presence of dowels, regardless of their type and quantity, did not exhibit any observable impact on the sensor signal.

Short-circuit detector. The short-circuit detector was developed using off-the-shelf electronic components. These components were then assembled and enclosed within a small 3cm cube box constructed out of plywood. The audio jack is positioned on the bottom of the box(Fig. 7B).

Signal processing and machine learning. Our approach to signal processing and machine learning followed the same method as described in iWood [30].

7 CONSTRUCTING A SMART TABLE USING WOODOWEL

To assess WooDowel as a material for the production of everyday objects, we organized a workshop where we invited an experienced woodworker to create a smart desk using WooDowel and our short-circuit detector.

Procedure. The woodworker was introduced to WooDowel panels and its application prior to the workshop. The goal of the workshop was for the participant to construct a desk using the WooDowel material. Although suggestions were given regarding possible dimensions for the desk's desktop, the woodworker had the freedom to make their own decisions throughout the crafting process. Eventually, the finalized design of the WooDowel desktop measured $1200mm \times 600mm$. Given that the primary use cases for WooDowel revolve around the detection of everyday objects on flat surfaces, our focus was solely on creating the desktop using WooDowel, while the legs of the desk were procured from a commercial source. To facilitate the cutting of the desktop, a table saw was provided to the woodworker. Following the completion of the cutting tasks, the participant proceeded to the assembly phase of the project. During the assembly phase, the woodworker drilled pilot holes in predetermined locations at the four corners of the desktop, where the screws for attaching the legs would be inserted. In the event of a short circuit detected by our detector, the participant replaced nearby dowels. Finally, the components were securely fastened together using screws (Fig. 12A). This process was successfully accomplished within approximately 20 minutes.

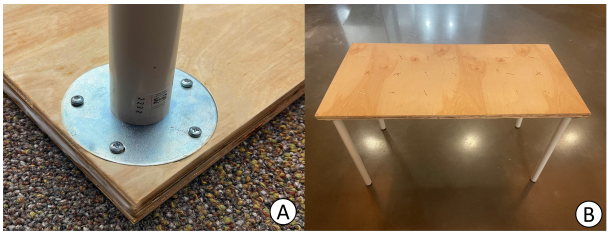

Figure 12: A: Attaching leg to the tabletop using screws. B: The finished table.

Result. Fig. 12B shows the assembled desk. The participant reported that the process of assembling this desk was not significantly different from their usual approach to creating a desk of a similar kind. During the assembly, the participant used a screwdriver to remove the connecting dowels and used either their finger or a hammer to facilitate the insertion of replacement regular wood dowels. A total of 4 connecting dowels were extracted during the process. Upon examining the sensor inside the completed desk, we found that all the affected electrodes were successfully detached from the main body of the sensor. Consequently, the remaining sensing area within the desktop accounted for 12.5% of its original size. In our interview with the participant, we discovered that although the task of dowel swapping was new to the assembly of a desk, it was familiar to them due to their experience in woodwork. Consequently, they found the task easy to perform. The process of replacing the connecting dowels was not perceived as a burden. Despite the addition of dowel swapping to the established assembly routine, it did not hinder the overall process or introduce significant physical and cognitive strain. This was largely attributed to the use of the short-circuit detector, which proved to be valuable in communicating the internal status of the plywood sensor.

8 EVALUATION

We conducted an experiment to assess the sensing performance of the smart table constructed using WooDowel. The primary goal of our study was to investigate whether the incorporation of overlapping electrodes with EM shielding could enhance the accurate recognition of user activities, particularly those involving devices that had been challenging for the previous iWood design [30].

8.1 Participants

A total of ten right-handed participants, consisting of six males and four females, were recruited for this study. The average age of the participants was 22 years.

8.2 Activities

In order to evaluate the accuracy of our implementation in recognizing activities tested with the previous method that utilizes non-overlapping electrodes, we included a total of 12 activities from the iWood [30]. These activities included a range of kitchen-related tasks, such as chopping, slicing, stirring, tenderizing, grating, and rolling dough, as well as non-kitchen activities like writing, erasing, stapling, pumping lotion, dispensing tape, and rotating a pencil sharpener (Fig. 13). Additionally, we included the activity of placing an empty glass on a coaster, which serves as an additional sample that involved weak signals. Given that these activities do not involve the use of electronic devices, we introduced seven new activities that specifically involve various types of electronic devices commonly found in a kitchen or hardware workshop. These activities include operating a vacuum cleaner, using a jigsaw, electric drill, and electric sander, typing on a mechanical keyboard, boiling water in an electric kettle, and playing audio through a speaker (Fig. 13). All tasks were performed on the smart table, which had a Alienware M18 R1 laptop on it. This setup aimed to simulate real-world EM disturbance situations.

8.3 Data collection

Prior to the experiment, participants were provided with a brief period to familiarize themselves with the activities. Throughout the data collection phase, participants were instructed to engage in tasks, either while standing or sitting, based on their individual comfort preferences. For activities that required minimal user movement, such as using the kettle and speaker, participants were asked to place the device on the table and turn it on. It should be noted that data collection for the kettle was initiated after the water had started boiling. Participants were not constrained in terms of how they performed the tasks. Since the sensor signal was significantly

Figure 13: The tested activities and their corresponding signals.

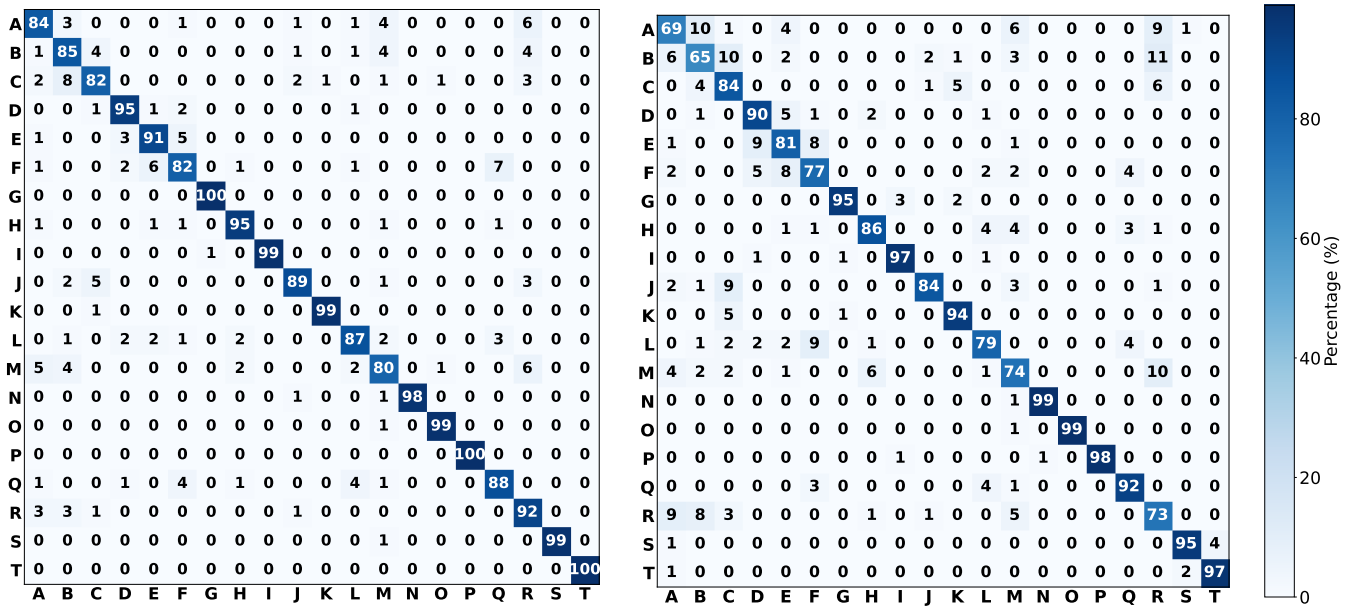

Figure 14: Left: within-user accuracy. Right: cross-user accuracy of the 20 tested activities.

weaker within the area of the isolated electrodes, activities could not be reliably detected within these regions. Hence, participants were asked to avoid the four corners of the desk where the isolated electrodes were located. However, there were no other restrictions on where the activities should occur within the remaining sensing area of the desk. Each participant completed ten repetitions of each activity, with the order of tasks randomized.

8.4 Result

In this section, we present the evaluation results of our system's recognition accuracy, which was assessed using within-user accuracy and cross-user accuracy.

8.4.1 Within-user Accuracy. The within-user accuracy of our smart table was assessed by measuring the prediction accuracy when the training and testing data were from the same user. To evaluate this accuracy, we performed twofold cross-validation for each participant. The results were averaged and presented in a confusion matrix (Fig. 14). Our analysis revealed that the mean within-user accuracy is 92.2% (std: 10.7%). Note that our system demonstrated high accuracy in recognizing activities involving electronic devices. However, there were certain activities that posed challenges for the system, leading to confusion in the predictions. Specifically, the activities of writing, erasing, pen sharpening, and typing were frequently misclassified. This confusion can be attributed to the fact that these activities generated vibration patterns primarily within a narrow low-frequency range (< 60Hz), resulting in relatively large overlaps. Additionally, activities characterized by a single and quick action, such as pumping, tape dispensing, and placing an empty glass on a coaster, posed more challenges for the system. The vibrations produced by these activities were transient and lacked distinct patterns, making them more difficult to differentiate accurately.

In addition to assessing the within-user accuracy of our smart table, we were interested in comparing its sensing performance to that of iWood [30]. To do so, we calculated the average within-user accuracy for the first twelve daily activities, which were also examined in iWood. It is important to note that our previous findings, as presented in Section 3.2, indicated that iWood struggled to achieve reasonable recognition accuracy without EM shielding. Therefore, when comparing our results with those of the iWood paper, it should be noted that the data from the iWood study represents the upper limit of iWood's performance, which is only achievable in an ideal environment free of EM interference. Notably, our implementation yielded a recognition accuracy of 91% (std: 7.6%), which was comparable to the reported accuracy of 94.7% in the iWood paper. We interpret our result as promising, particularly when considering the inclusion of an additional eight activities in our classifier.

8.4.2 Cross-user Accuracy. We also calculated the cross-user accuracy to assess the performance of our general model across multiple users. We employed a leave-one-subject-out cross-validation test, using data from nine participants for training and reserving the remaining participant's data for testing. Our results indicate that, on average, the model achieved a cross-user accuracy of 86.4% (std: 11.7%). The corresponding confusion matrix is displayed in Fig. 14. Upon further examination, we observed an increase in confusion among the activities that were already problematic for the system, such as writing, erasing, pen sharpening, and typing. Additionally, vacuuming the table began to be misclassified alongside these activities. This outcome can be attributed to the fact that different participants exhibited variations in their writing, erasing, and typing, making it more challenging for the system to differentiate between these activities, particularly those with vibration patterns within a narrow band in the frequency range below 60Hz.

Furthermore, the classification of pumping, tape dispensing, and placing a glass also deteriorated, as different users applied varying degrees of force during these actions. However, it is worth noting that our model maintained a high accuracy of over 95% (std: 4.9%)

for activities involving electronic devices, excluding the vacuum. This high level of accuracy can be attributed to the fact that these activities are less influenced by user-specific behavior, allowing for more consistent and accurate recognition.

Additionally, we calculated the average cross-user accuracy for the first twelve activities, which yielded a result of 83.4%. This accuracy is comparable to the 87.8% observed in the iWood system, which again was obtained in a less realistic environment devoid of EM interference. These findings are encouraging, particularly considering that our sensor design allows for the recognition of activities involving electronic devices in an environment with EM noise.

9 LIMITATION AND FUTURE WORK

We present insights learned from this work, discuss the limitations of our prototype, and propose future research.

9.1 Improving Vibration Sensing

Our investigation has revealed that our plywood sensor faces challenges in distinguishing activities with similar vibration patterns, especially in the low-frequency range. This issue is further amplified when these activities occur simultaneously. To address this challenge, one potential approach is to enhance the sensor's sensitivity and resolution, thereby magnifying the discernible differences between the signals of these activities. Previous research has demonstrated the potential of utilizing chemical or physical methods to increase the frequency response of triboelectric sensors [1, 4, 24]. For instance, Fan et al. [4] used PTFE polymer nanowires to boost charge density in the sensor to enhance its sensitivity. In our future research, we will employ similar techniques to enhance our sensor's sensitivity and improve its sensing accuracy.

9.2 Sensing During Woodworking

Currently, our system includes a short-circuit detector to warn woodworkers for manually isolating the electrodes. However, this detector holds the potential for future upgrades that could monitor a broader range of activities and track woodworking progress using the plywood sensor. This is feasible because the detector has continuous access to real-time sensor data and can track signals accordingly. By incorporating machine learning algorithms into the detector, it can offer more interactive experiences for woodworkers when they use the plywood sensor to create smart furniture. For instance, the detector could record the sequence of woodworking processes, thereby generating data that could be useful for woodworkers who wish to create a tutorial for his fabrication steps. Additionally, based on data collected from experienced woodworkers, the system could offer context-rich guidance and step-by-step instructions to help novices successfully complete their projects.

9.3 Sensor Segmentation

Our smart table now functions as a single, unified sensor for detecting the vibrations caused by user activities. It is a basic feature for non-technical woodworkers to use WooDowel in their projects. However, by manually separating the electrodes and connecting them using multiple power jack dowels, the sensor can actually be segmented into a sensor array, empowering the sensing system to infer the locations of user activities. This could be a valuable feature for technically-inclined woodworkers to build a more advanced smart furniture. As we look to the future, we plan to develop a system to also guide non-technical users to handle the segmentation of the sensor to achieve more advanced applications.

9.4 Manual Operation

In our initial attempt to redesign the plywood vibration sensor, we aimed to address the most pressing issues by incorporating manual interventions from woodworkers. While our approach demonstrated potential in isolating electrodes affected by short circuits, the reliance on manual operation for the isolation process could potentially be replaced with more efficient techniques. Thus, our future research will focus on exploring methods that can empower the plywood sensor to autonomously identify and isolate the affected electrode as soon as a short circuit is detected.

9.5 Error Detection and Repair

Once the plywood sensor has been deployed in the physical environment, troubleshooting and identifying issues causing malfunctions becomes a complex task, primarily due to the fact that the electrodes are concealed within the plywood. In our lab, we resorted to manually inspecting each electrode to address such problems, but this approach is neither practical nor feasible for end users in a real-world setting. Moreover, fixing the identified issues poses even greater challenges, particularly considering that the plywood sensor is already incorporated as an integral part of furniture or flooring. Given these challenges, our future research will focus on exploring hardware and software tools to facilitate the process of debugging and resolving hardware-related issues in the plywood sensor. We aim to develop more efficient and effective means for users to address malfunctions to ensure the practicality and usability of the plywood sensor in real-world applications.

9.6 Recycling

When comparing our prototype to pure wooden items that can easily decompose or be incinerated, it becomes apparent that our incorporation of metal and plastic components poses potential challenges to the decomposition and disposal processes. These additional materials complicate the natural breakdown of the item and may contribute to environmental pollution if not properly managed. In light of this, our future research will explore alternative conductive materials that are more environmentally friendly, with the aim of replacing the current sensing elements using copper. By doing so, we strive to align our design more closely with sustainable design principles.

9.7 Dowel Locking Mechanism

The implementation of our current prototype can be improved in several different ways. One potential avenue for such improvement involves investigating the integration of a locking mechanism, such as a push lock, to ensure the secure positioning of the dowel within its designated hole. Note that in instances where a dowel positioned along the edge of a plywood panel is damaged by cutting, it can no longer be effectively anchored within the broken dowel hole. However, the electrical connections of its electrodes will remain

unaffected through the functional dowels at the remaining corners. To restore the visual appeal of the edge, the damaged hole can be fixed by using wood filler.

10 CONCLUSION

In this research, we unveiled WooDowel, an innovative strategy tailored to confront the unique challenges associated with maintaining the functionality of triboelectric vibration sensors embedded in smart plywood during woodworking operations that utilize nails and screws. While traditional sensor designs have consistently displayed vulnerabilities when exposed to electromagnetic interference, particularly in real-world applications, WooDowel presents a transformative solution. This is achieved by facilitating manual isolation of short-circuited electrodes. As a result, WooDowel not only fortifies the inherent signal strength of the sensors but also significantly augments their resilience against external interferences. This amalgamation of features leads to a substantial enhancement in user activity recognition capabilities. Through rigorous empirical evaluations, we have reaffirmed the prowess of WooDowel. In practical applications, our prototype has consistently demonstrated an outstanding recognition accuracy that exceeds 90%, underscoring the potential of this novel approach in the realm of smart woodworking applications.

REFERENCES

[1] Nivedita Arora, Steven L. Zhang, Fereshteh Shahmiri, Diego Osorio, Yi-Cheng Wang, Mohit Gupta, Zhengjun Wang, Thad Starner, Zhong Lin Wang, and Gregory D. Abowd. 2018. SATURN: A Thin and Flexible Self-Powered Microphone Leveraging Triboelectric Nanogenerator. *Proc. ACM Interact. Mob. Wearable Ubiquitous Technol.* 2, 2, Article 60 (jul 2018), 28 pages. https://doi.org/10.1145/3214263

[2] Artem Dementyev, Hsin-Liu Kao, and Joseph A Paradiso. 2015. Sensortape: Modular and programmable 3d-aware dense sensor network on a tape. In *Proceedings of the 28th Annual ACM Symposium on User Interface Software & Technology*. 649–658.

[3] Xing Fan, Jun Chen, Jin Yang, Peng Bai, Zhaoling Li, and Zhong Lin Wang. 2015. Ultrathin, rollable, paper-based triboelectric nanogenerator for acoustic energy harvesting and self-powered sound recording. *ACS nano* 9, 4 (2015), 4236–4243.

[4] Xing Fan, Jun Chen, Jin Yang, Peng Bai, Zhaoling Li, and Zhong Lin Wang. 2015. Ultrathin, Rollable, Paper-Based Triboelectric Nanogenerator for Acoustic Energy Harvesting and Self-Powered Sound Recording. *ACS Nano* 9, 4 (April 2015), 4236–4243. https://doi.org/10.1021/acsnano.5b00618 Publisher: American Chemical Society.

[5] Jun Gong, Yu Wu, Lei Yan, Teddy Seyed, and Xing-Dong Yang. 2019. Tessutivo: Contextual interactions on interactive fabrics with inductive sensing. In *Proceedings of the 32nd Annual ACM Symposium on User Interface Software and Technology*. 29–41.

[6] Saifei Hao, Jingyi Jiao, Yandong Chen, Zhong Lin Wang, and Xia Cao. 2020. Natural wood-based triboelectric nanogenerator as self-powered sensing for smart homes and floors. *Nano Energy* 75 (2020), 104957.

[7] Ahmed Haroun, Mohamed Tarek, Mohamed Mosleh, and Farouk Ismail. 2022. Recent progress on triboelectric nanogenerators for vibration energy harvesting and vibration sensing. *Nanomaterials* 12, 17 (2022), 2960.

[8] Chris Harrison and Scott E Hudson. 2008. Scratch input: creating large, inexpensive, unpowered and mobile finger input surfaces. In *Proceedings of the 21st annual ACM symposium on User interface software and technology*. 205–208.

[9] David Holman and Roel Vertegaal. 2011. TactileTape: low-cost touch sensing on curved surfaces. In *Proceedings of the 24th annual ACM symposium adjunct on User interface software and technology*. 17–18.

[10] Te-Chien Hou, Ya Yang, Hulin Zhang, Jun Chen, Lih-Juann Chen, and Zhong Lin Wang. 2013. Triboelectric nanogenerator built inside shoe insole for harvesting walking energy. *Nano Energy* 2, 5 (2013), 856–862.

[11] Kiyoshi Itao. 2007. Wearable Sensor Network Connecting Artifacts, Nature and Human Being. In *SENSORS, 2007 IEEE*. 1120–1123. https://doi.org/10.1109/ICSENS.2007.4388603

[12] Weon-Guk Kim, Do-Wan Kim, Il-Woong Tcho, Jin-Ki Kim, Moon-Seok Kim, and Yang-Kyu Choi. 2021. Triboelectric nanogenerator: Structure, mechanism, and applications. *Acs Nano* 15, 1 (2021), 258–287.

[13] Saman Kuntharin, Viyada Harnchana, Jirapan Sintusiri, Prasit Thongbai, Annop Klamchuen, Kitiphat Sinthiptharakoon, Vittaya Amornkitbamrung, and Prinya Chindaprasirt. 2023. Smart triboelectric floor based on calcium silicate-carbon composite for energy harvesting and motion sensing applications. *Sensors and Actuators A: Physical* 358 (2023), 114423.

[14] Zhihui Lai, Junchen Xu, Chris R Bowen, and Shengxi Zhou. 2022. Self-powered and self-sensing devices based on human motion. *Joule* 6, 7 (2022), 1501–1565.

[15] Long Lin, Sihong Wang, Yannan Xie, Qingshen Jing, Simiao Niu, Youfan Hu, and Zhong Lin Wang. 2013. Segmentally structured disk triboelectric nanogenerator for harvesting rotational mechanical energy. *Nano letters* 13, 6 (2013), 2916–2923.

[16] Jinming Ma, Yang Jie, Jie Bian, Tao Li, Xia Cao, and Ning Wang. 2017. From triboelectric nanogenerator to self-powered smart floor: a minimalist design. *Nano Energy* 39 (2017), 192–199.

[17] E Wood Meier. 2015. Identifying and using hundreds of woods worldwide. *Wood Database* (2015).

[18] Simiao Niu, Sihong Wang, Long Lin, Ying Liu, Yu Sheng Zhou, Youfan Hu, and Zhong Lin Wang. 2013. Theoretical study of contact-mode triboelectric nanogenerators as an effective power source. *Energy & Environmental Science* 6, 12 (2013), 3576–3583.

[19] Simiao Niu and Zhong Lin Wang. 2015. Theoretical systems of triboelectric nanogenerators. *Nano Energy* 14 (2015), 161–192. https://doi.org/10.1016/j.nanoen.2014.11.034 Special issue on the 2nd International Conference on Nanogenerators and Piezotronics (NGPT 2014).

[20] Simon Olberding, Nan-Wei Gong, John Tiab, Joseph A Paradiso, and Jürgen Steimle. 2013. A cuttable multi-touch sensor. In *Proceedings of the 26th annual ACM symposium on User interface software and technology*. 245–254.

[21] Shijia Pan, Ceferino Gabriel Ramirez, Mostafa Mirshekari, Jonathon Fagert, Albert Jin Chung, Chih Chi Hu, John Paul Shen, Hae Young Noh, and Pei Zhang. 2017. Surfacevibe: vibration-based tap & swipe tracking on ubiquitous surfaces. In *Proceedings of the 16th ACM/IEEE International Conference on Information Processing in Sensor Networks*. 197–208.

[22] Patrick Parzer, Florian Perteneder, Kathrin Probst, Christian Rendl, Joanne Leong, Sarah Schuetz, Anita Vogl, Reinhard Schwoediauer, Martin Kaltenbrunner, Siegfried Bauer, et al. 2018. Resi: A highly flexible, pressure-sensitive, imperceptible textile interface based on resistive yarns. In *Proceedings of the 31st Annual ACM Symposium on User Interface Software and Technology*. 745–756.

[23] Yu Shao, Xinyue Wang, Wenjie Song, Sobia Ilyas, Haibo Guo, and Wen-Shao Chang. 2021. Feasibility of using floor vibration to detect human falls. *International journal of environmental research and public health* 18, 1 (2021), 200.

[24] Jianguo Sun, Kunkun Tu, Simon Büchele, Sophie Marie Koch, Yong Ding, Shivaprakash N. Ramakrishna, Sandro Stucki, Hengyu Guo, Changsheng Wu, Tobias Keplinger, Javier Pérez-Ramírez, Ingo Burgert, and Guido Panzarasa. 2021. Functionalized wood with tunable tribopolarity for efficient triboelectric nanogenerators. *Matter* 4, 9 (2021), 3049–3066. https://doi.org/10.1016/j.matt.2021.07.022

[25] Saiganesh Swaminathan, Jonathon Fagert, Michael Rivera, Andrew Cao, Gierad Laput, Hae Young Noh, and Scott E Hudson. 2020. Optistructures: Fabrication of room-scale interactive structures with embedded fiber bragg grating optical sensors and displays. *Proceedings of the ACM on Interactive, Mobile, Wearable and Ubiquitous Technologies* 4, 2 (2020), 1–21.

[26] Ryo Takahashi, Takuya Sasatani, Fuminori Okuya, Yoshiaki Narusue, and Yoshihiro Kawahara. 2018. Design of Cuttable Wireless Power Transfer Sheet. In *Proceedings of the 2018 ACM International Joint Conference and 2018 International Symposium on Pervasive and Ubiquitous Computing and Wearable Computers*. 456–459.

[27] Wei Teng, Xian Ding, Shiyao Tang, Jin Xu, Bingshuai Shi, and Yibing Liu. 2021. Vibration analysis for fault detection of wind turbine drivetrains—A comprehensive investigation. *Sensors* 21, 5 (2021), 1686.

[28] Zhong Lin Wang. 2013. Triboelectric nanogenerators as new energy technology for self-powered systems and as active mechanical and chemical sensors. *ACS nano* 7, 11 (2013), 9533–9557.

[29] Raphael Wimmer and Patrick Baudisch. 2011. Modular and deformable touch-sensitive surfaces based on time domain reflectometry. In *Proceedings of the 24th annual ACM symposium on User interface software and technology*. 517–526.

[30] Te-Yen Wu and Xing-Dong Yang. 2022. iWood: Makeable Vibration Sensor for Interactive Plywood. In *Proceedings of the 35th Annual ACM Symposium on User Interface Software and Technology*. 1–12.

[31] Robert Xiao, Greg Lew, James Marsanico, Divya Hariharan, Scott Hudson, and Chris Harrison. 2014. Toffee: enabling ad hoc, around-device interaction with acoustic time-of-arrival correlation. In *Proceedings of the 16th international conference on Human-computer interaction with mobile devices & services*. 67–76.

[32] Minyi Xu, Peihong Wang, Yi-Cheng Wang, Steven L Zhang, Aurelia Chi Wang, Chunli Zhang, Zhengjun Wang, Xinxiang Pan, and Zhong Lin Wang. 2018. A soft and robust spring based triboelectric nanogenerator for harvesting arbitrary directional vibration energy and self-powered vibration sensing. *Advanced Energy Materials* 8, 9 (2018), 1702432.

[33] Jin Yang, Jun Chen, Ying Liu, Weiqing Yang, Yuanjie Su, and Zhong Lin Wang. 2014. Triboelectrification-based organic film nanogenerator for acoustic energy

harvesting and self-powered active acoustic sensing. *ACS nano* 8, 3 (2014), 2649–2657.

[34] Yuanming Zeng, Huijing Xiang, Ning Zheng, Xia Cao, Ning Wang, and Zhong Lin Wang. 2022. Flexible triboelectric nanogenerator for human motion tracking and gesture recognition. *Nano Energy* 91 (2022), 106601.

[35] Hulin Zhang, Ya Yang, Yuanjie Su, Jun Chen, Katherine Adams, Sangmin Lee, Chenguo Hu, and Zhong Lin Wang. 2014. Triboelectric nanogenerator for harvesting vibration energy in full space and as self-powered acceleration sensor. *Advanced Functional Materials* 24, 10 (2014), 1401–1407.